Thermal Defocusing of a CO_2 Laser Beam in Air Doped With SF_6

LOUIS SICA AND E. A. MCLEAN

High Temperature Physics Branch
Plasma Physics Division

July 15, 1970

NAVAL RESEARCH LABORATORY
Washington, D.C.

CONTENTS

ABSTRACT

The transient aspects of the thermal defocusing of a CO_2 laser beam (10.6 μ) propagating through air doped with SF_6 have been studied using an infrared detector and interferometry. A comparison of these results with theory has shown that the defocusing occurring in air is qualitatively similar to that observed at 0.63 μ in liquid CCl_4 doped with iodine.

PROBLEM STATUS

This is the final report on one phase of a continuing problem.

AUTHORIZATION

NRL Problem K03-08A
ARPA Order 660

Manuscript submitted March 24, 1970.

THERMAL DEFOCUSING OF A CO_2 LASER BEAM IN AIR DOPED WITH SF_6

INTRODUCTION

This report presents a laboratory study of thermal defocusing in air using a CO_2 laser beam. Our philosophy in undertaking a small-scale experiment is to gain sufficient understanding of the phenomenon to predict the results of larger scale field experiments and to indicate the areas where the efforts with the larger and more expensive experiments should be concentrated. There are several advantages to performing a laboratory experiment rather than a field experiment if one wants to gain an understanding of the field situation. For example, beam quality, absorption coefficient, path length, wind velocity, and the homogeneity of the medium can be controlled. The medium itself can be varied as well as the beam diameter so as to change the time constants associated with conduction and convection effects. Since one can limit the number of interactions in the phenomenon, a theoretical description of the effects of each independent variable taken separately becomes feasible. Approximate theories for limiting cases may be more easily tested and generated. These separate analyses may then enable one to understand the more complex situation for which a purely mathematical analysis might be exceedingly difficult.

OBSERVATIONS

Intensity Profiles

The observations which we report here are of two different types which are designed to supplement each other. The first is the observation of the intensity profile of the defocusing beam as a function of time. The second is the observation, versus time, of the integrated index of refraction perpendicular to the defocusing beam. These observations clarify the processes of conduction and convection along the beam.

Figure 1 shows the experimental arrangement used to observe the intensity profile of the defocusing beam. The CO_2 laser beam had a power of 3.2 W and a power density at the center of 21 W/cm^2. It passed through a cell 16 cm in length which contained one atmosphere of air and enough SF_6 (less than 5 torr) to provide an absorption coefficient of 0.087 cm^{-1}. This is not enough to alter the bulk properties of the medium from those of air. The beam was then swept in a vertical plane past a gold-doped germanium detector by a four-sided rotating mirror moving at 1800 rpm.

The rotating mirror and the detector were also used to measure the Gaussian parameter of the laser beam as it entered the absorption cell. (The Gaussian parameter is defined here as the half width of the intensity profile at 1/e.) Figure 2 shows the measured laser intensity profile scaled to fit a Gaussian function. The good fit ensures that the laser was operating in the TEM_{00} mode. The Gaussian parameter β for the laser beam was found to be 0.22 cm.

Figure 3 shows the intensity profile of the defocusing beam at the indicated times measured from the moment of opening of an electromechanical shutter. A pulse from the shutter triggers the upper sweep of an oscilloscope, which is shown as the upper

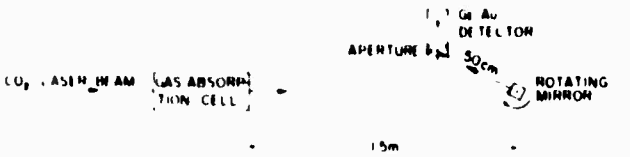

Fig. 1 - Apparatus for the determination of the laser beam profile.

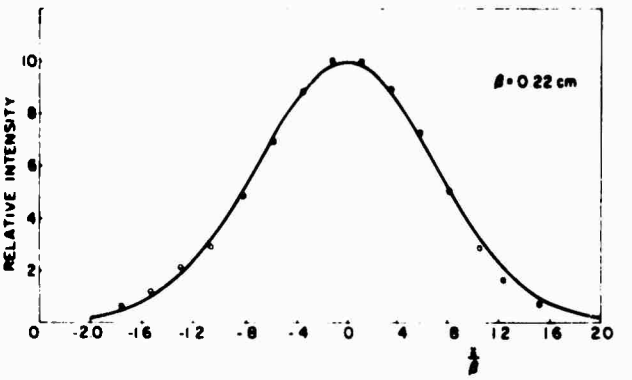

Fig. 2 - Laser intensity profile at 3.8 W. The data points are experimental measurements and the curve is a theoretical Gaussian (e^{-x^2/β^2}).

trace in each picture. Each spike on the upper trace corresponds to one sweep of the defocusing beam across the detector. After a variable time delay, a brightened spike occurs, which is magnified by the faster speed of the lower sweep. One can see from the upper trace spikes on the first oscillogram that the defocusing reaches a maximum (or the peak intensities reach a minimum) at about 0.05 sec. After attaining its maximum diameter the beam contracts somewhat, but not to its original width. This is shown by the increase in amplitude of the spikes of the upper trace in the last frame at 0.44 sec. It is also shown clearly by the increase in height and decrease in width of the pattern in the lower trace of this frame when compared with the beam profile shown in the immediately preceding frames. This lessening of defocusing is caused by increased convection which brings unheated air into the beam path, thus increasing the refractive index of the medium; this has been observed previously in thermal defocusing in liquids by Carman and Kelley (1). Due to the vertical plane of the scan across the detector face one observes one peak instead of the two peaks corresponding to a half moon rim. We have observed the half-moon pattern, however, in the defocused beam using a liquid crystal detector.

Index of Refraction

We turn now to the observation of the index of refraction changes which cause the defocusing. The arrangement of the apparatus for these observations is shown in Fig. 4. The CO_2 laser beam is incident on a beam expander which, for the present experiment, was operated one-to-one, i.e., both mirrors had equal focal lengths. The mirrors were adjusted so that there was slight focusing of the beam to reduce its diameter somewhat

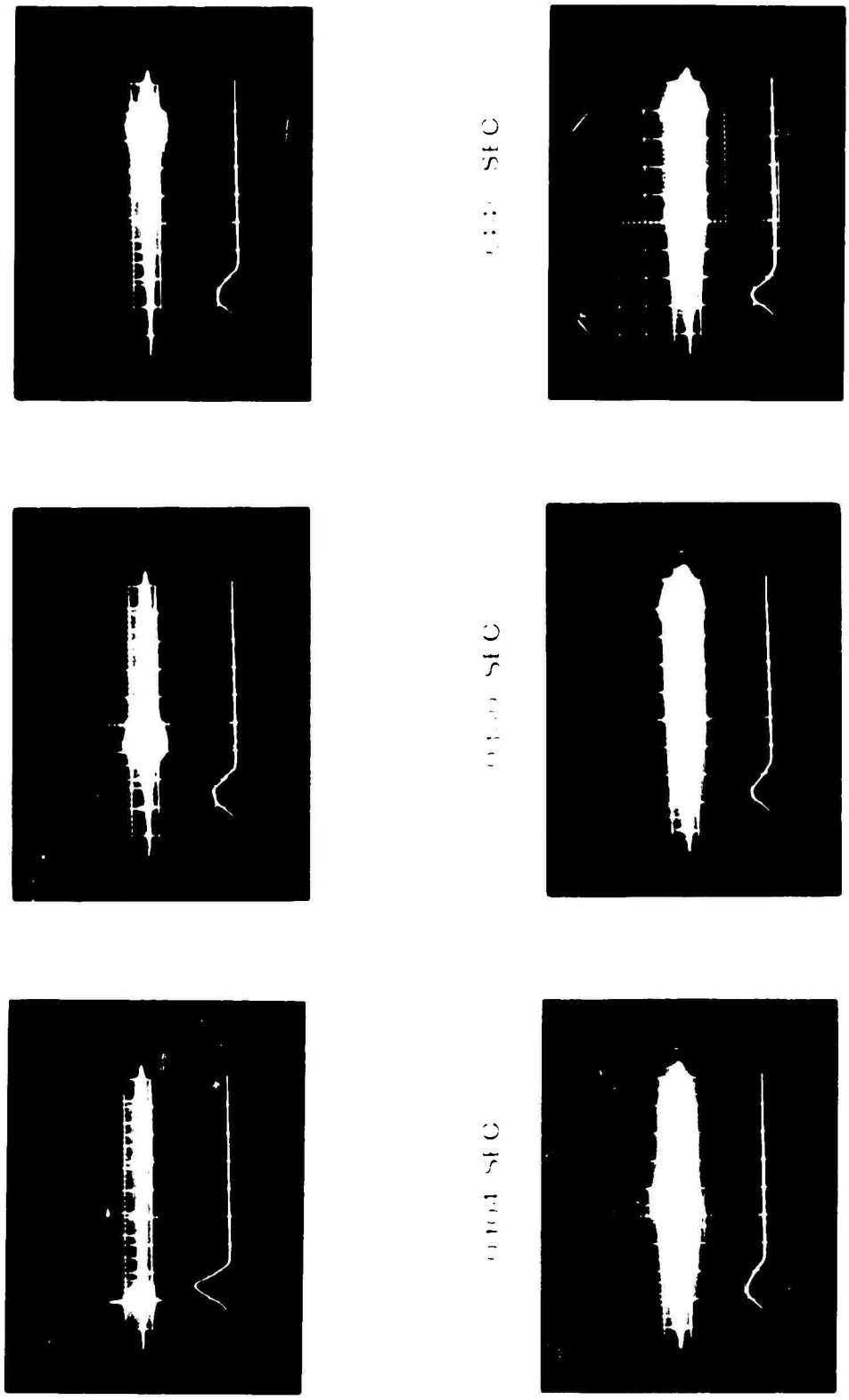

Fig. 3. – Intensity scans of defocusing laser beam. The times shown indicate the time that has elapsed since opening of the camera shutter.

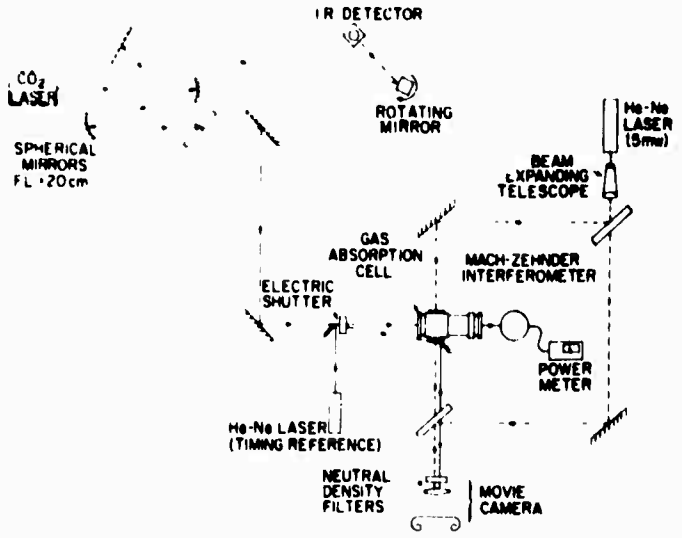

Fig. 4 - Experimental arrangement for observing interferometer fringes.

at the cell entrance window located 4 m from the laser. The dashed mirror after the beam expander was used to deflect the beam to a rotating mirror and then to a detector for measurement of its profile. The distance from the mirror to the detector equaled that from the mirror to the cell. The timing reference laser sent a beam into the field of view of the movie camera when the shutter opened, thus marking a zero reference time. The power meter was used to monitor continuously the power during each filming run. The 5-mW He-Ne laser in the upper right-hand corner served as the light source for the Mach-Zehnder interferometer.

Before considering the movie data of the fringes formed during defocusing in air, it is useful for purposes of comparison to review briefly the evolution of the fringes accompanying defocusing of a He-Ne laser beam in liquid carbon tetrachloride doped with iodine (2). This is shown in Fig. 5. The defocusing beam itself is shown at the right of the fringes at corresponding times. Notice that at 0.5 and 0.9 sec the fringes and the defocusing beam are essentially symmetrical. At 2.5 sec the defocusing beam has almost reached its steady-state asymmetry, but the fringe asymmetry is only perceptible in the very first fringe at the left. In the bottom frame (6.8 sec) a cylinder of heated fluid is rising in the cell, but the defocusing beam has not changed appreciably.

The movie in the case of CO_2 absorption in air was taken at 500 frames/sec but, except for the faster rate of development, the evolution of the fringes is observed to be similar to that described above. Three frames from this reel, representing states corresponding to the last three frames shown in Fig. 5 for liquid CCl_4, are shown in Fig. 6. The defocusing beam is incident from the left at the position indicated by the arrow. The early time symmetry of the fringes gives way to gradually increasing asymmetry as the fringes move upward in the field of view due to increasing convection. Cooler air replaces the heated air and there is a decrease in the amplitude of fringe deflection along the heating beam axis.

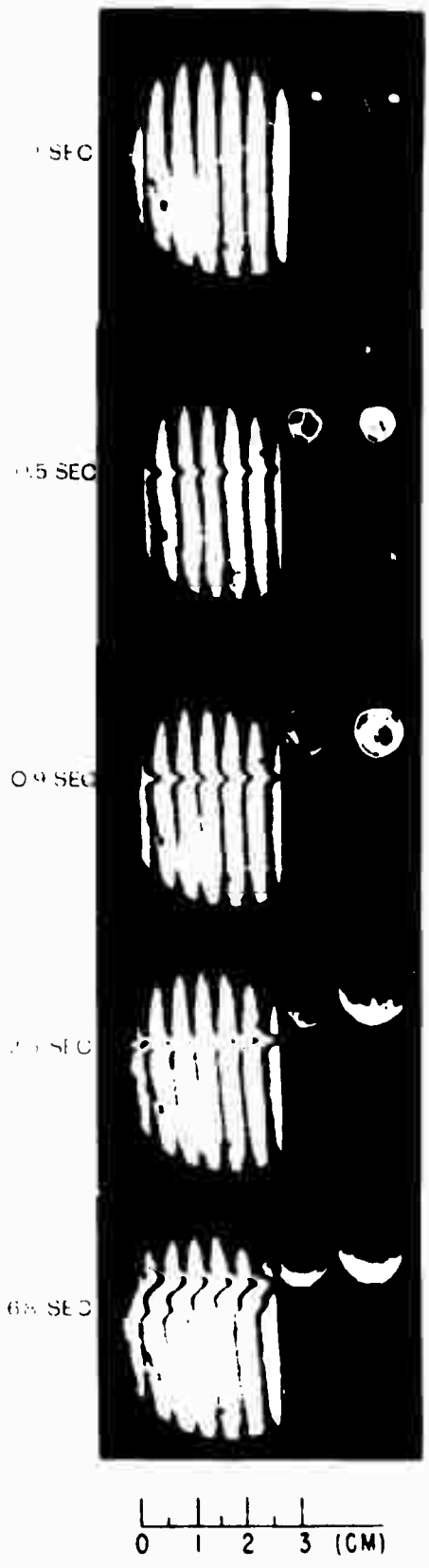

Fig. 5 - Interference fringe deflection due to the heating of CCl_4 by the absorption of He-Ne laser light (6328 Å). The heating beam passes through the cell horizontally from left to right. The time indicated on the left of each photograph is the time elapsed since turning on the laser beam. The two small patterns at the right show the thermally defocused laser beam as viewed 55 cm from the exit window of the liquid cell. (Two patterns are produced due to reflections from the two surfaces of the beam splitter.)

Fig. 6 - Selected frames taken from a movie showing the interference fringe deflection due to heating of air (doped with SF_6) by the absorption of CO_2 laser light (10.6 μ). The time elapsed since turning on the laser beam is (a) 0.011 sec, (b) 0.159 sec, and (c) 0.275 sec. The heating laser beam (arrow) enters the absorption cell through a window and passes horizontally through the cell from left to right. (The dot in the lower right-hand corner of the frames is from the timing reference laser.)

DATA ANALYSIS

We have exploited the similarity between the liquid and gas cases by fitting fringe shapes occurring at early times to contours computed from the thermal diffusion equation alone, under the assumption of a Gaussian heating source (2). Figure 7 shows such a fit for a fringe ~1 cm from the entrance window at 0.042 sec. The dashed line on this figure indicates the shape of the Gaussian heat source used to compute the shape of the outer curve. The reasonable fit of the data is consistent with the general indication that convection is a small influence at this time.

Figure 8 is a composite of the shapes assumed by the fringe at a set of different times. These times are listed on each curve. It is pertinent to consider the shape of the fringe at significant times in the evolution of the defocusing as indicated by the rotating mirror intensity data. In Fig. 8 a fringe at 0.05 sec would correspond to maximum defocusing. Perceptible upward fringe motion is beginning to occur at about that time, which also corresponds to the thermal conduction time. The thermal conduction time constant $\tau_c = 4K$ (where K is the heat diffusivity) equals 0.056 sec for our beam radius. (The conduction time is the time it takes for a heat impulse to spread over the beam

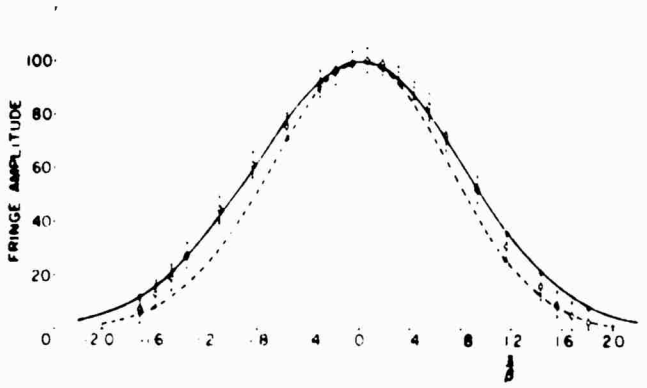

Fig. 7 - Fringe shape in air doped with SF_6 where τ_c $^{-2}$ 4K 0.0576 sec and t 0.012 sec. Measured values are plotted together with their estimated error brackets. Solid line is a theoretical curve. The dashed line is the Gaussian heat source.

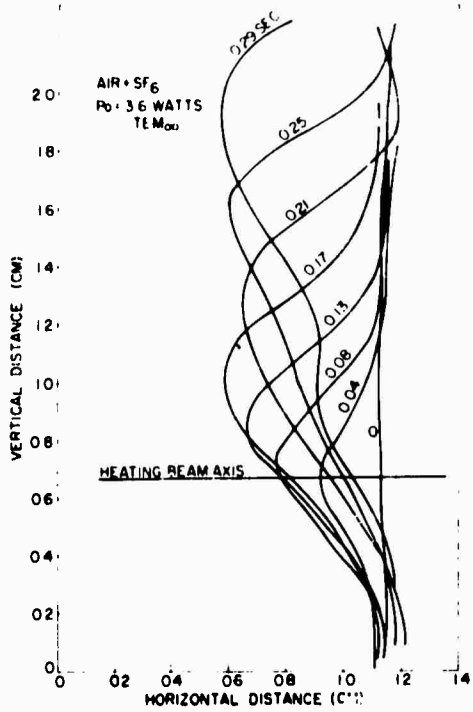

Fig. 8 - Composite fringe shapes at different times during thermal defocusing in air doped with SF_6.

area and, in the convectionless case, it corresponds to the time at which the beam has defocused to about half its maximum size.) Contraction of the defocusing beam has been completed by about 0.29 sec so that the fringe at that time corresponds to a steady state for the propagation process. The fringes in the region of the heating beam have essentially reached their final shape. Consequently, the fluid motion need be accounted for theoretically only during a limited time and over the limited region of the heating beam.

Another indication of the nature of the fluid motion is shown in Fig. 9. This is a plot of the vertical displacement x of the fringe peak versus time. The plot indicates that although fluid motion begins at t = 0, the displacement has been less than 25% of the Gaussian parameter up to about 0.05 sec. As we have seen, the defocusing stops increasing after this time because of the increase in the fluid motion. The shape of the graph appears to be roughly parabolic and the log-log plot of Fig. 10 shows that this is indeed the case. The equation of the curve of best fit is shown in the upper left-hand corner of Fig. 10.

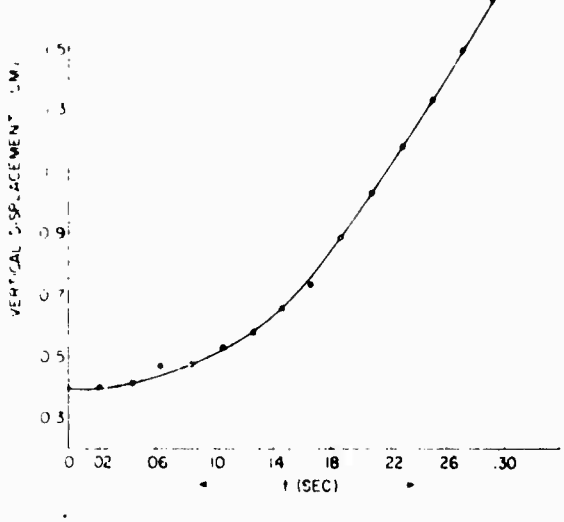

Fig. 9 - Vertical displacement of the fringe peak as a function of time.

We have computed the position of an elemental volume of the heated fluid versus time as it rises in the cell, using an approximate solution to the Navier-Stokes equation. The resulting expression for the displacement D at early times t is

$$D = \frac{1}{6T} \frac{g I_0 \alpha t^3}{\rho c_p},$$

where g is the acceleration of gravity, T is the absolute temperature, α is the absorption coefficient, I_0 is the intensity at the center of the beam, ρ is the density, and c_p is the specific heat at constant pressure. From this expression, one can estimate the length of time for which convection is negligible for beams of various powers and diameters, and for different absorption coefficients. For example, for two beams with different diameters propagating through media with absorption coefficients α_1 and α_2, the times t_2 and t_1 at which the displacements correspond to equal fractions of a beam diameter D/3 are related by

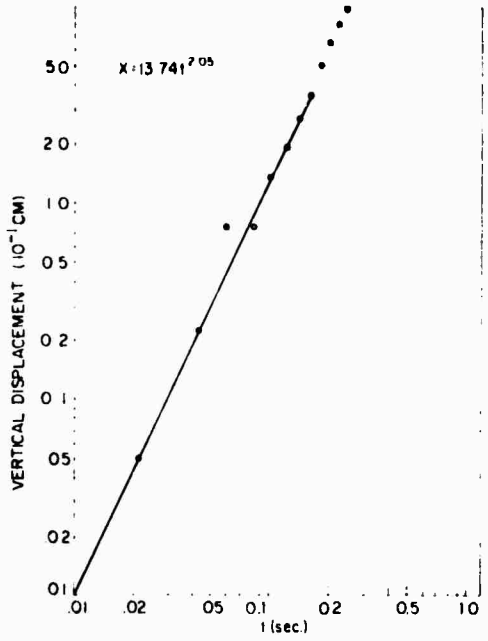

Fig. 10 - Log-log plot of vertical displacement of the fringe peak as a function of time.

$$t_2 = \left(\frac{I_1 \alpha_1 \beta_2}{I_2 \alpha_2 \beta_1}\right)^{1/3} t_1 .$$

Using the values obtained from the present experiment for the quantities with the subscript 1, and 0.05 secs for t_1 as the latest time for which convection could be neglected, a corresponding time can be computed for the case of propagation of wide laser beams in the atmosphere for the zero-velocity case.

If convection can be neglected, one may describe defocusing through the use of the aberrationless theory given by Akhmanov et al. (3). The Akhmanov equation can be optimally tested by observing thermal defocusing in ethylene glycol since the viscosity of this liquid is such that convection does not enter into the effect. Figure 11 shows a log-log plot of the Gaussian parameter divided by its zero-time value versus time, for a defocusing beam after transversing a cell of ethylene glycol and a small amount of dye. The curve was determined from a computer solution of the Akhmanov et al. equation shown at the right. The square root dependence on time of beam defocusing reported by Carman and Kelley (1) can be obtained from this equation. The experimental points were obtained by measuring the intensity versus time at the center of the defocusing beam. As may be seen, the experimental points fit the theoretical curve quite well. This result, together with the interferometric data presented above, indicates that the Akhmanov equation may be used to generate graphs of defocusing versus distance at times short compared to the convection time for the case of propagation in the atmosphere.

In summary, our experiments have shown the strong similarity between thermal defocusing in liquids and gases. Consequently, much of the theory that has been developed for the liquids case can be applied to the gas case also.

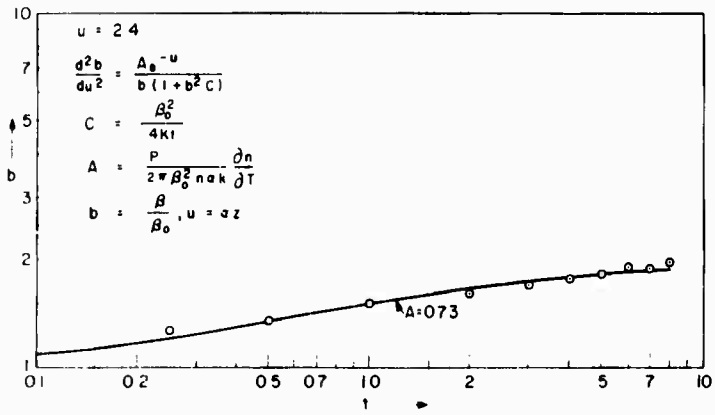

Fig. 11 - Log-log plot of the normalized Gaussian parameter b for a defocusing He-Ne laser beam in ethylene glycol plus a small amount of dye. The data points are derived from experimental measurements of intensity at the center of the beam, and the solid line is calculated from the solution of the Akhmanov et al. equation at various times.

REFERENCES

1. Carman, R.L., and Kelley, P.L., Appl. Phys. Letters 12:241 (1968).

2. McLean, E.A., Sica, L., and Glass, A.J., Appl. Phys. Letters 13:369 (1968).

3. Akhmanov, S.A., Krindach, D.P., Migulin, A.V., Sukhorukov, A.P., and Khokhlov, R.V., IEEE J. Quant. Elect., QE-4:568 (1968).

Security Classification

DOCUMENT CONTROL DATA - R & D

(Security classification of title, body of abstract and indexing annotation must be entered when the overall report is classified)

1. ORIGINATING ACTIVITY *(Corporate author)*

Naval Research Laboratory
Washington, D.C. 20390

2a. REPORT SECURITY CLASSIFICATION

Unclassified

2b. GROUP

3. REPORT TITLE

THERMAL DEFOCUSING OF A CO_2 LASER BEAM IN AIR DOPED WITH SF_6

4. DESCRIPTIVE NOTES *(Type of report and inclusive dates)*

Final report on one phase of a continuing problem.

5. AUTHOR(S) *(First name, middle initial, last name)*

Louis Sica and E.A. McLean

6. REPORT DATE	7a. TOTAL NO. OF PAGES	7b. NO. OF REFS
July 15, 1970	14	3

8a. CONTRACT OR GRANT NO.	9a. ORIGINATOR'S REPORT NUMBER(S)
NRL Problem K03-08A	
b. PROJECT NO.	NRL Problem 7107
ARPA Order 660	
c.	9b. OTHER REPORT NO(S) *(Any other numbers that may be assigned this report)*
d.	

10. DISTRIBUTION STATEMENT

This document has been approved for public release and sale; its distribution is unlimited.

11. SUPPLEMENTARY NOTES	12. SPONSORING MILITARY ACTIVITY
	Advanced Research Projects Agency, Washington, D.C.

13. ABSTRACT

The transient aspects of the thermal defocusing of a CO_2 laser beam (10.6 μ) propagating through air doped with SF_6 have been studied using an infrared detector and interferometry. A comparison of these results with theory has shown that the defocusing occurring in air is qualitatively similar to that observed at 0.63 μ in liquid CCl_4 doped with iodine.

DD FORM 1 NOV 68 1473 (PAGE 1)

S/N 0101-807-6801

Security Classification

14 KEY WORDS	LINK A		LINK B		LINK C	
	ROLE	WT	ROLE	WT	ROLE	WT
Carbon dioxide lasers						
Laser beams						
Air						
Carbon tetrachloride						
Thermal measurements						
Interferometers						
Nonlinear optics						
Optical propagation						